J. Phys.: Condens. Matter 5 (1993) 8425–8436. Printed in the UK

Kondo behaviour in Ce–Si amorphous alloys

Takehiko Hihara†, Kenji Sumiyama†, Hiroshi Yamauchi†, Yoshiya Homma†, Takashi Suzuki‡ and Kenji Suzuki†

† Institute for Materials Research, Tohoku University, Sendai 980, Japan
‡ Department of Physics, Tohoku University, Sendai 980, Japan

Received 20 April 1993, in final form 12 July 1993

Abstract. Incoherent Kondo effects have been observed in Ce_xSi_{100-x} ($x = 18$, 53, 66 and 87) amorphous alloys produced by sputtering. They show large enhancement of the electronic specific-heat coefficient at low temperatures, being classified as heavy-fermion systems. The magnetic susceptibility reveals a Curie–Weiss law at $T > 100$ K with an effective Bohr magneton number of about $2.45\mu_B$. However, the electrical resistivity is large, revealing a Kondo-type logarithmic temperature dependence. The atomic randomness prohibits the coherent Kondo state and the formation of a magnetically ordered state in the Ce–Si amorphous alloys.

1. Introduction

Recently a great deal of interest has been centred on heavy-fermion phenomena in cerium, ytterbium and uranium alloy systems which have f electrons hybridized with conduction electrons and strongly correlated with each other [1]. These systems show an extremely large specific-heat coefficient at low temperatures, a transition from a Kondo-type logarithmic to a low-temperature T^2 variation in the electrical resistivity and a transition from Curie–Weiss to enhanced Pauli-paramagnetic behaviour in the magnetic susceptibility. These anomalous properties have been ascribed to the Fermi-liquid degeneracy in the periodic crystalline systems [2, 3]. However, deep understanding of such heavy-fermion systems has been hindered by the differences in the crystal structures and limited solution ranges of these intermetallics.

For the amorphous alloys, on the other hand, we can study the concentration dependence of the physical properties without any structure change and elucidate the effect of atomic disorder on heavy-fermion systems. In previous papers [4], we have reported the production of Ce–Cu amorphous alloys and their incoherent Kondo behaviour; the extremely large electronic specific-heat coefficient occurs because of the reduction in the Kondo temperature.

The $CeSi_{1.86}$ intermetallic compound [5] shows a dense Kondo behaviour with a rather high T_K ($\sim$ 20 K). Numerous recent experimental studies have elucidated the low-temperature properties of the $CeSi_x$ alloys ($1.60 < x < 2.00$) with the α-$ThSi_2$-type structure. These $CeSi_x$ compounds show enhancement of the electronic specific-heat coefficient $\gamma(0)$ at 0 K from 104 to 240 mJ mol^{-1} K^{-2}, a Kondo-type electrical resistivity and a non-magnetic-to-ferromagnetic transition.

Ce–Si amorphous alloys have already been produced by co-evaporation onto a liquid-nitrogen-cooled substrate [6], showing a spin-glass-like magnetic transition at low temperatures. However, no systematic study has been done, probably because of the very small sizes of specimens produced by co-evaporation. Therefore we have produced bulk Ce–Si amorphous alloys by high-rate sputter deposition.

In the previous publications, we have mentioned the basic low-temperature properties of the Ce_xSi_{100-x} ($x = 18$ and 66) amorphous alloys [7] and a comparative study between amorphous and crystallized $Ce_{66}Si_{34}$ alloys [8]. These Ce–Si amorphous alloys are also classified as heavy-fermion systems, because the electronic specific-heat coefficient γ is extremely large in contrast with no enhancement for the γ-value of $La_{66}Si_{34}$ amorphous alloy with no f electrons. In this report, we deal with the concentration dependence of low-temperature physical properties of Ce_xSi_{100-x} amorphous alloys.

2. Experimental procedures

Alloy targets were prepared by arc melting in an Ar gas atmosphere using 99% pure cerium and 99.999% pure silicon. Thin plates of about 300 μm thickness were prepared on water-cooled Cu substrates in a DC triode sputtering equipment. After elimination of the Cu substrate by mechanical polishing, the chemical compositions were determined by gravimetric analysis.

The structure factors $S(Q)$ of the Ce_xSi_{100-x} amorphous alloys were obtained by a conventional x-ray diffraction technique within a 2θ range from 3.5 to 140° using Mo Kα radiation monochromated by curved graphite. The differential scattering calorimetry (DSC) trace was measured between 400 and 1000 K.

The low-temperature specific heat was measured between 1.8 and 30 K by a conventional heat-pulse method with a mechanical heat switch in an adiabatic cell. The magnetic susceptibility was measured between 5 and 290 K using a torsion balance magnetometer in a magnetic field of up to 9.5 kOe. The magnetization was also measured at 4.2 and 1.8 K using an extracting magnetometer in a magnetic field of up to 150 kOe. With a DC four-probe method the electrical resistivity was measured between 2.5 and 300 K. The magnetoresistance was also measured at 4.2 K in longitudinal magnetic fields up to 140 kOe.

3. Results

Figure 1 shows the total structure factor $S(Q)$ of as-prepared Ce_xSi_{100-x} alloys observed by x-ray diffraction, where $Q = (4\pi \sin\theta)/\lambda$ and λ is the wavelength of the Mo Kα radiation. A halo pattern due to amorphous phase formation is predominant and the vibration amplitude of $S(Q)$ attenuates in the high-Q region. The DSC trace of the as-sputtered alloys displayed clear exothermic peaks, indicating crystallization of the amorphous phase. These results clearly demonstrate that the present alloys are amorphous. The crystallization temperatures T_X, defined as the starting point of the exothermic peak, are presented in table 1. T_X increases with decreasing concentration x of Ce.

Figure 2 shows the specific heat C_p per mole of Ce atoms for the as-sputtered Ce_xSi_{100-x} alloys. C_p increases slightly with decreasing temperature below 10 K and reveals a broad peak at around $T = 4$ K for Ce_xSi_{100-x} amorphous alloys with $x = 53$ and 66. In order to clarify this anomalous behaviour, C_p/T normalized to a mode of Ce atoms is plotted as a function of T^2 in figure 3. C_p/T for all the present alloys rapidly increases with decreasing temperature below $T \simeq 10$ K, and the C_p/T for $x = 53$ and 66 shows clear peaks at $T = 3.2$ K and 2.7 K, respectively, as observed for the crystalline Ce_5Si_3 compound [9]. The ground-state electronic specific-heat coefficients estimated by linear extrapolation to 0 K of C_p/T versus T^2 plots for $T < 5$ K are about 1100 mJ mol^{-1} K^{-2}, 450 mJ mol^{-1} K^{-2}, 600 mJ mol^{-1} K^{-2} and 950 mJ mol^{-1} K^{-2} for $x = 18$, 53, 66 and 87,

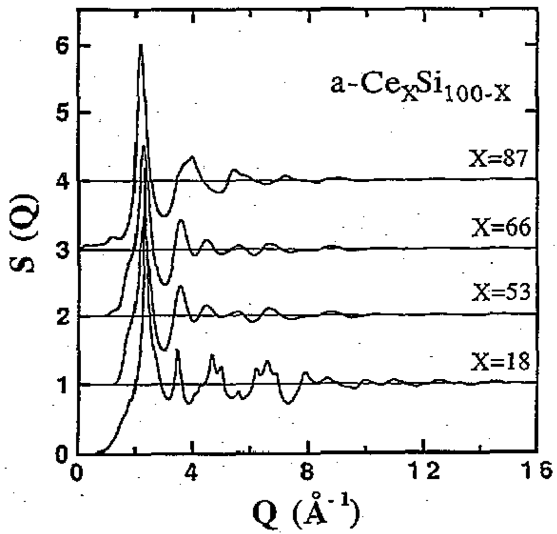

Figure 1. Total structure factors $S(Q)$ of sputter-deposited Ce_xSi_{100-x} alloys.

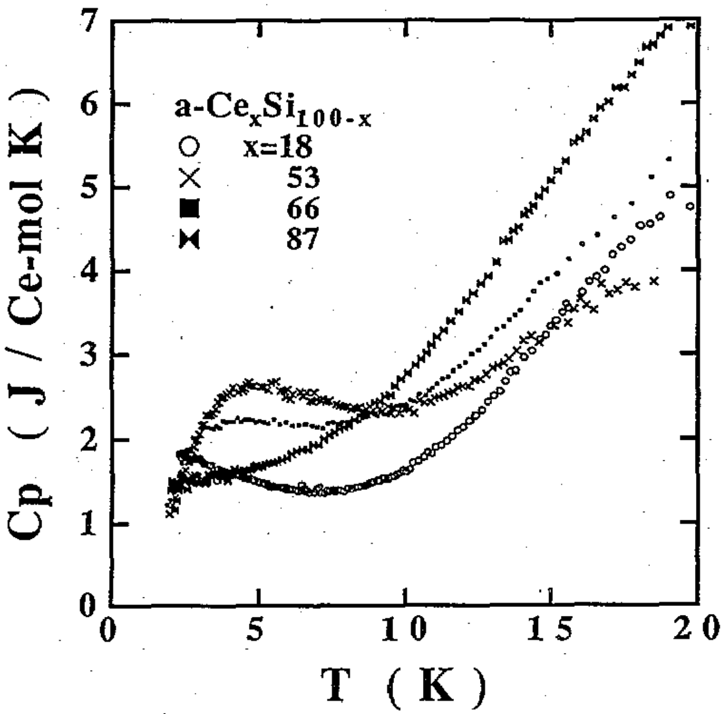

Figure 2. Specific heat C_p at constant pressure normalized to a mole of Ce atoms as a function of temperature T for Ce_xSi_{100-x} amorphous alloys.

respectively, and are much larger than those of the intermetallic $CeSi_{1.86}$ [5] and Ce_5Si_3, which are 203 mJ mol^{-1} K^{-2} and 250 mJ mol^{-1} K^{-2}, respectively. Figure 4(a) shows the apparent electronic specific-heat coefficient $\gamma(0)$ estimated from the high-temperature

Table 1. Physical properties of Ce_xSi_{100-x} amorphous alloys. The crystallization temperature T_X is defined as the starting point of the exothermic peak of DSC plots. The electronic *specific heat coefficient $\gamma(0)$ is estimated from the high-temperature part ($T > 10$ K) of the C_p/T versus T^2 plots. The ground-state susceptibility $\chi(0)$ is extrapolated from* χ versus T plots. The high-field susceptibility $\chi_{HF}(0)$ is estimated from the high-field ($H > 100$ kOe) region by linear extrapolation from $M(H)$ curves at 1.8 K. The effective Bohr magneton numbers μ_{eff} and μ'_{eff} are estimated from the high-temperature ($T > 100$ K) and low-temperature ($T < 30$ K) parts, respectively, of χ^{-1} versus T plots. The Curie–Weiss temperature is denoted Θ. The spontaneous magnetization M_s is found by linear extrapolation to $H = 0$ from $M(H)$ curves at 1.8 K for $H > 100$ kOe. The Wilson ratio R is calculated from equation (1).

x in Ce_xSi_{100-x}	T_X (K)	$\gamma(0)$ (mJ (mol Ce)$^{-1}$ K^{-2})	$\chi(0)$ (emu (mol Ce)$^{-1}$)	μ_{eff} (μ_B)	μ'_{eff} (μ_B)	Θ (K)	$\chi_{HF}(0)$ (emu (mol Ce)$^{-1}$)	M_s (μ_B/Ce atom)	R
18	779	169	0.098	2.45	1.77	−26	0.0063	0.62	1.4
53	723	177	0.19	2.44	2.05	−15	0.0067	0.74	1.4
66	634	206	0.14	2.43	1.81	−24	0.0066	0.59	1.2
87	527	288	0.066	2.46	2.00	−53	0.0080	0.38	1.0

parts of these C_p/T versus T^2 plots for $T > 10$ K. The $\gamma(0)$-values for all the present alloys increase with increasing x and are much larger than that of La_5Si_3 [8]. This clearly indicates that the present alloys are heavy-fermion systems.

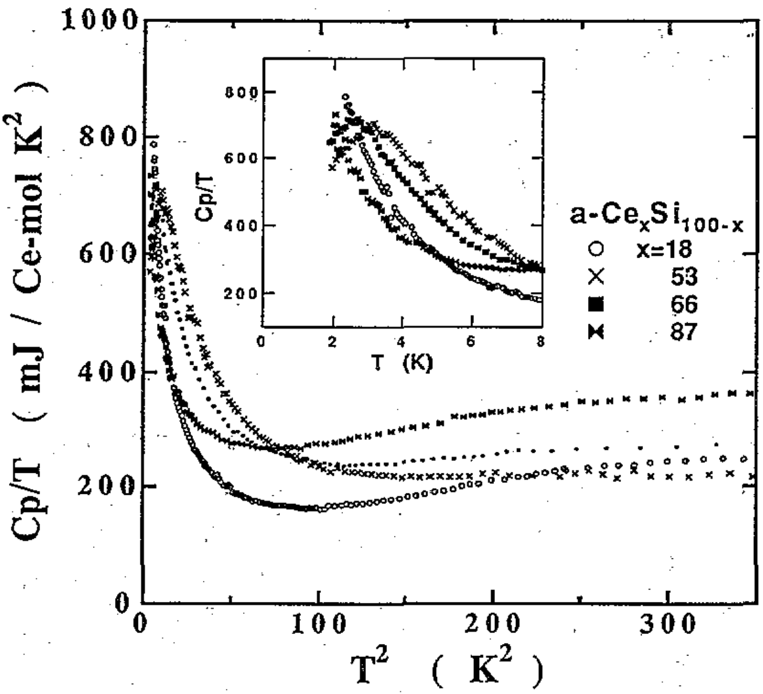

Figure 3. C_p/T versus T^2 plots for Ce_xSi_{100-x} amorphous alloys.

Figure 5 shows the magnetic susceptibility χ and χ^{-1} normalized to a mole of Ce atoms at $H = 9.5$ kOe as functions of temperature T. The χ^{-1} versus T curves for the present alloys roughly obey the Curie–Weiss law between 30 and 300 K. They deviate downwards from the straight line below 30 K and become nearly constant below 10 K. Figure 4(*b*) shows the effective Bohr magneton numbers μ_{eff} and μ'_{eff} of Ce atoms estimated from the Curie–Weiss constant for 100 K $< T <$ 300 K and 10 K $< T <$ 30 K, respectively. μ_{eff} is slightly smaller than the theoretical value of $2.54\mu_B$ for Ce^{3+} f^1 and the results of $(2.6–2.65)\mu_B$ for crystalline $CeSi_{1.86}$ compounds, but larger than the result of $2.38\mu_B$ for the crystalline Ce_5Si_3 compound. Figure 4(*c*) shows the ground-state susceptibility $\chi(0)$ obtained by extrapolation to 0 K of the χ versus T plots for $T < 10$ K. They are much larger than that of the crystalline compounds of $CeSi_{1.86}$, also showing a maximum value for $x = 53$. Figure 6 presents the magnetization M versus the magnetic field H curves at $T = 4.2$ and 1.8 K for the present alloys. M increases non-linearly with increasing H below 100 kOe but shows a linear H dependence above 100 kOe. Figure 4(*c*) shows the high-field magnetic susceptibility $\chi_{HF}(0)$ estimated from the linear portion of the $M(H)$ curves at $T = 1.8$ K for $H > 100$ kOe. $\chi_{HF}(0)$ increases with increasing x. Figure 4(*a*) presents the relationship between the spontaneous magnetization M_s, as found by extrapolating the slope of $T = 1.8$ K for the high-field region ($H > 100$ kOe) to $H = 0$ and Ce content. M_s also shows a maximum value at $x = 53$.

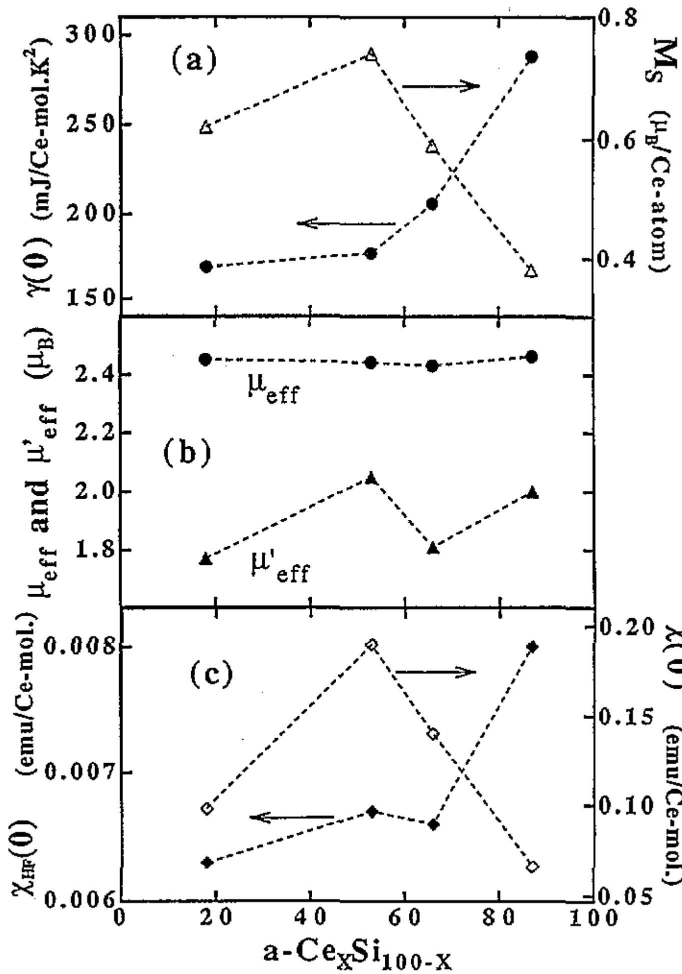

Figure 4. Relationships between (*a*) the electronic specific-heat coefficient $\gamma(0)$, the spontaneous magnetization M_s, (*b*) the effective Bohr magneton numbers μ_{eff} and μ'_{eff}, (*c*) the ground-state susceptibility $\chi(0)$ and the high-field susceptibility $\chi_{HF}(0)$, which are given in table 1, and the Ce content of Ce_xSi_{100-x} amorphous alloys.

Figure 7(*a*) shows the electrical resistivity $\rho(T)$ for the present alloys. $\rho(T)$ is very large, indicating a very short mean free path of conduction electrons in the amorphous state. $\rho(T)$ is insensitive to T for $T > 20$ K except for $x = 18$. As shown in figure 7(*b*), $\rho(T)/\rho(300\text{ K})$ for $x = 18$, 53 and 66 slightly follows a $-\log T$ dependence below 30 K: the incoherent impurity Kondo effect. $\rho(T)$ for the $CeSi_{1.86}$ intermetallic compound gradually decreases with decreasing T down to 50 K, drops rapidly below 50 K and reveals a T^2 dependence, indicating the formation of the Kondo lattice. $\rho(T)/\rho(300\text{ K})$ for $x = 87$ is independent of T for the measured temperature range. The temperature dependence for $x = 18$, on the other hand, exponentially increases down to 15 K and logarithmically increases below 15 K being similar to the behaviour in an impurity semiconductor as shown in figure 8.

Figure 9 shows the magnetoresistance $\Delta\rho(H)/\rho(0)$ as a function of the longitudinal magnetic field H for the as-sputtered alloys. Here $\Delta\rho(H) = \rho(H) - \rho(0)$; $\rho(H)$ is the

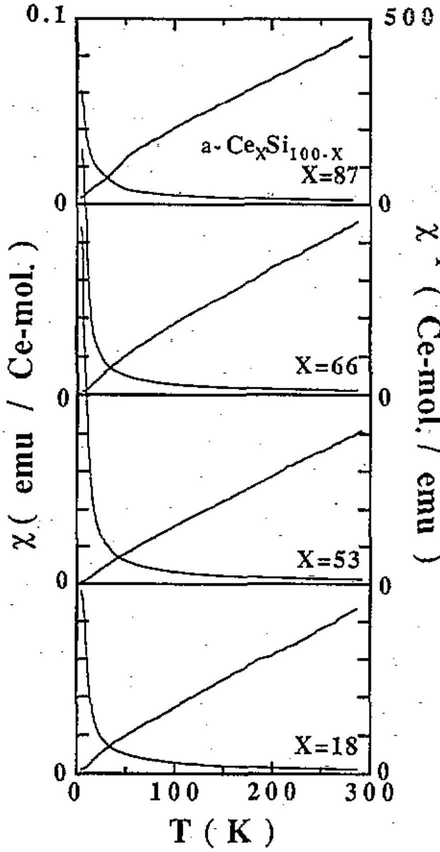

Figure 5. Magnetic susceptibility χ and inverse magnetic susceptibility χ^{-1} as functions of temperature T for Ce_xSi_{100-x} amorphous alloys. Here, χ and χ^{-1} are normalized to a mole of Ce atoms.

resistivity at $H \neq 0$ and $\rho(0)$ is that at $H = 0$. The $\Delta\rho(H)/\rho(0)$-values are about one order smaller than those of the crystalline counterparts [10]. For $x = 66$, $\Delta\rho(H)/\rho(0)$ is slightly positive below 20 kOe and changes its sign to negative between 20 and 120 kOe and to positive up to 140 kOe. $\Delta\rho(H)/\rho(0)$ is negative for $x = 18$ and 53; however, $\Delta\rho(H)/\rho(0)$ is positive for $x = 87$.

4. Discussion

The electronic specific-heat coefficients $\gamma(0)$ of Ce_xSi_{100-x} amorphous alloys are extremely large compared with those of transition-metal amorphous alloys. Such high values of the electronic specific-heat coefficients must originate from the 4f electrons in Ce atoms, because no enhancement was observed in the γ-value of the sputter-deposited La_5Si_3 amorphous alloy which has no f electrons [8]. Therefore the electronic density of states is enhanced at the Fermi level due to the Kondo resonance, i.e. the Ce_xSi_{100-x} amorphous alloys are classified as heavy-fermion systems.

In several Ce intermetallic compounds in which non-magnetic third elements randomly occupy the Ce atom sites, disordering is introduced around the Ce ions and causes a variation in RKKY interactions [11]. In such cases, a Schottky-like anomaly appears in the heat capacity at very low temperatures owing to the splitting of the low-lying crystal-field levels. They also display a clear peak in χ at low temperatures, which can be ascribed to a spin-glass state originating from random Ce–Ce exchange interactions. The C_p/T

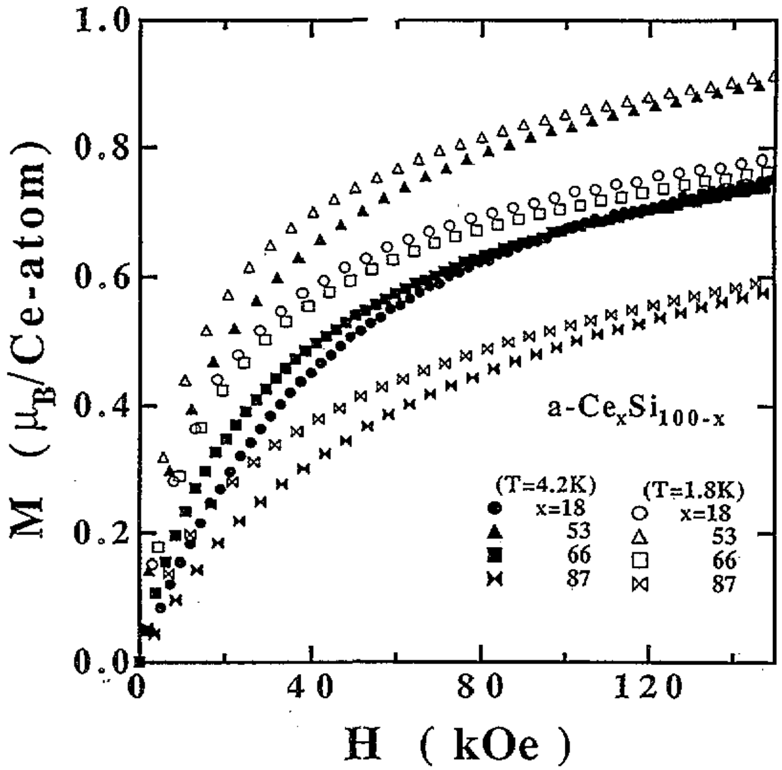

Figure 6. Magnetization curves at 4.2 K and 1.8 K of Ce_xSi_{100-x} amorphous alloys.

versus T^2 variation in Ce_xSi_{100-x} ($x = 53$ and 66) amorphous alloys exhibits clear peaks at $T = 3.2$ K and 2.7 K, respectively, where the peak in the C_p/T versus T^2 plots for $x = 66$ roughly coincides with that for the crystalline counterpart Ce_5Si_3. The Ce_5Si_3 compound has a tetragonal Cr_5B_3-type structure constituted of two Ce atom sites (Ce^I and Ce^{II}) in the unit cell. The nearest neighbour of Ce^{II} in Ce_5Si_3 forms a dimer, giving rise to singlet ground and triplet excited states because 4f electrons of the dimers (which are the ground doublet state) are coupled to each other by antiferromagnetic exchange [9]. The peak in the C_p/T versus T^2 plots has been ascribed to a Schottky-type specific heat due to the splitting between the singlet and triplet.

The electrical resistivity of Ce_xSi_{100-x} amorphous alloys is very large as it is due to defect and disorder scattering, which is characteristic for amorphous alloys. It logarithmically increases at low temperatures, indicating an impurity Kondo system. This logarithmic dependence in $\rho(T)$ can be observed at lower temperatures with increasing x, and $\rho(T)$ for $x = 87$ reveals no logarithmic dependence. Moreover, $\rho(T)$ of the present alloys does not display a T^2-dependence down to 2.5 K, indicating no Kondo lattice formation.

In ion-irradiated $CeCu_2Si_2$, $CeCu_6$ and UPt_3 [12], the temperature T^* at which $\rho(T)$ reveals a low-temperature maximum is depressed by several lattice defects. Since the $\rho(T)$ of the present amorphous alloy is consistent with this phenomenon, T_K of the present amorphous alloys shifts to low temperatures in comparison with those for their crystalline counterparts, because the lattice disordering causes destruction of coherence in the quasi-particle state and a localization effect.

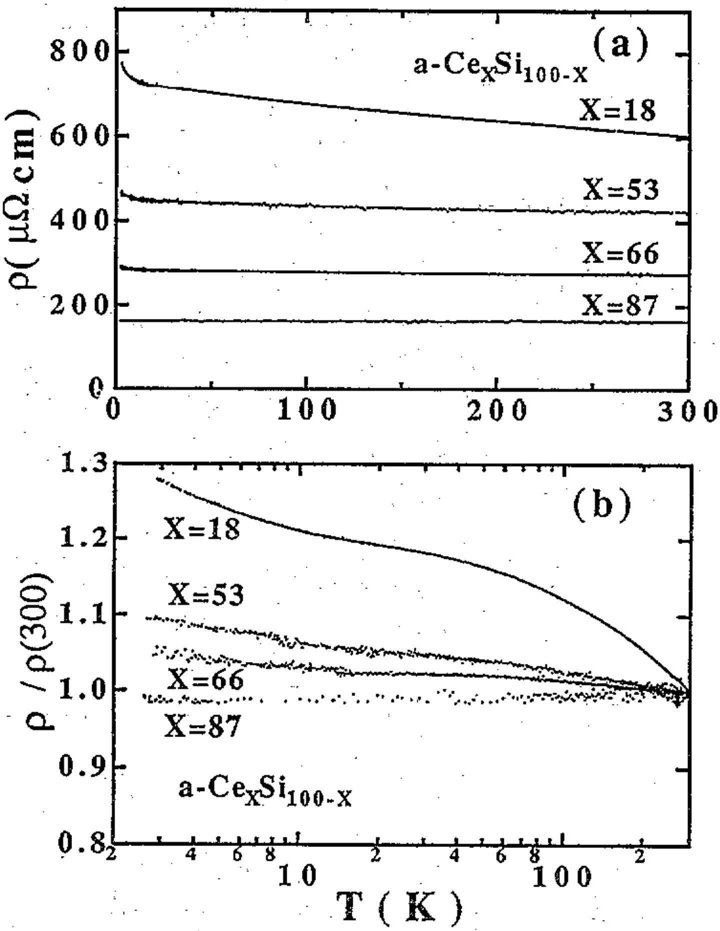

Figure 7. (*a*) Temperature dependence of the electrical resistivity $\rho(T)$ and (*b*) relative change $\rho(T)/\rho(300\ \mathrm{K})$ in the electrical resistivity as a function of $\log T$ for Ce_xSi_{100-x} amorphous alloys.

Measurement of the magnetoresistance $\Delta\rho(H)/\rho(0)$ is also important because it reflects the transition between incoherent and coherent scattering in heavy-fermion systems [2, 13]. In an incoherent Kondo system [14], a magnetically ordered system [15] and a spin-glass state [16], $\Delta\rho(H)/\rho(0)$ is negative because the magnetic moments are aligned by the magnetic field, reducing electron scattering. In a coherent Kondo system, on the other hand, the skew scattering of conduction electrons is enhanced at low magnetic fields showing a positive $\Delta\rho(H)/\rho(0)$ as in simple metals.

The variations in $\Delta\rho(H)/\rho(0)$ for the present Ce_xSi_{100-x} amorphous alloys are very small compared with the crystalline counterparts [10]. It is reasonable to suppose that $\Delta\rho(H)/\rho(0)$ for an amorphous alloy is smaller than that for the crystalline counterpart because it has a large residual resistivity and the Fermi surface is more isotropic than that for a crystalline alloy [17]. The sign of $\Delta\rho(H)/\rho(0)$ is negative for $x = 18$, 53 and 66, but positive for $x = 87$ at 4.2 K. When these results are combined with the temperature dependence of electrical resistivity, the logarithmic temperature dependence of $\rho(T)$ for $x = 18$, 53 and 66 is ascribed to incoherent Kondo effect, where the Kondo temperatures

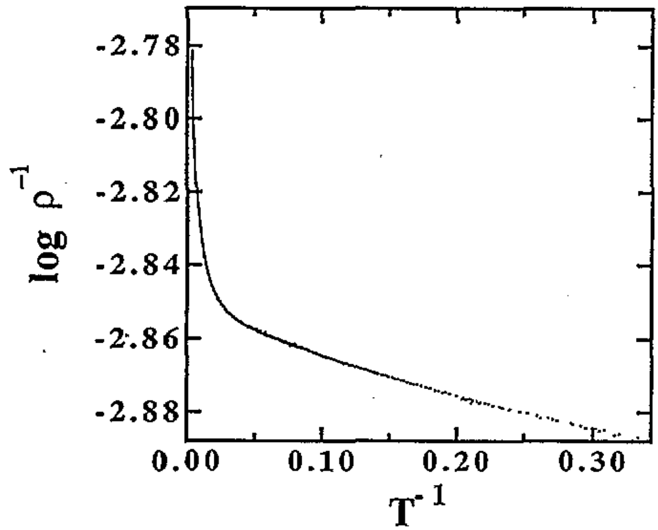

Figure 8. Relationship between $\log \rho(T)^{-1}$ and T^{-1} for Ce_xSi_{100-x} amorphous alloys with $x = 18$.

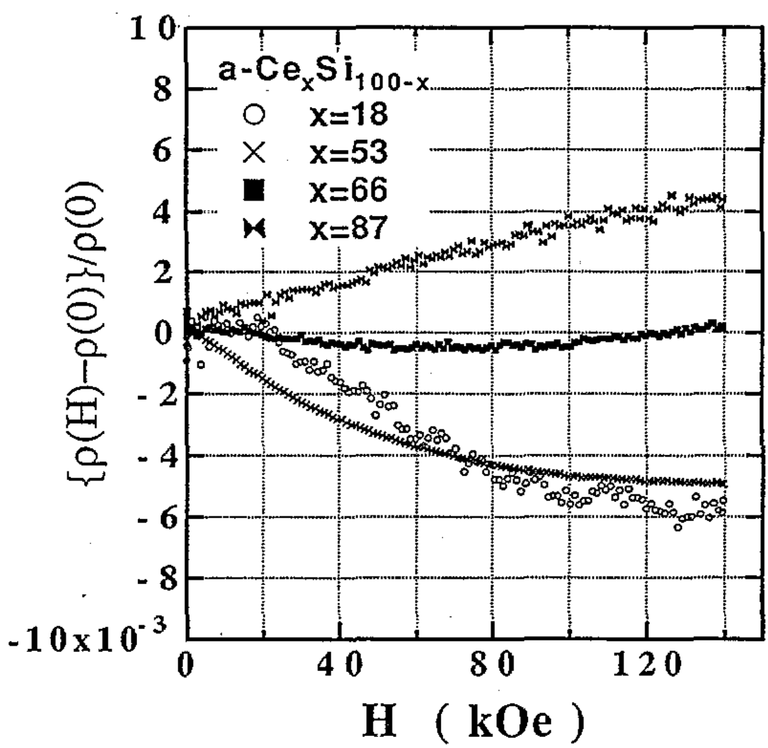

Figure 9. Magnetoresistance $\Delta\rho(H)/\rho(0)$ as a function of applied longitudinal magnetic field H at 4.2 K for Ce_xSi_{100-x} amorphous alloys.

become lower than that of the crystalline counterpart. The logarithmic temperature dependence of $\rho(T)$ at low temperatures is not observed for $x = 87$, probably because the Kondo temperature is lower than the observed temperature range. This behaviour is consistent with its positive magnetoresistance at 4.2 K; the metallic contribution (positive) dominates the incoherent Kondo contribution (negative) in the temperature range which is higher than the Kondo temperature. With increasing x, T_K becomes lower and $\gamma(0)$ increases, where $\gamma(0)$ is inversely proportional to the T_K [3]. However, it is plausible that the $Ce_{18}Si_{82}$ amorphous alloy is like a semiconductor, because the temperature coefficient of resistivity is large and negative. As shown in figure 8 ($\ln \rho^{-1}$ versus T^{-1} curve: an Arrhenius plot), the gap energy of the $Ce_{18}Si_{82}$ amorphous alloy is estimated to be 1×10^{-3} eV for $T > 50$ K, and 2×10^{-5} eV for $T < 10$ K. These values are much smaller than the gap of pure Si (1.14 eV).

A relationship (Wilson ratio) between the zero-temperature susceptibility $\chi(0)$ and the linear coefficient $\gamma(0)$ of the specific heat has been derived for heavy-fermion systems [18]:

$$R = \pi^2 k_B^2 \chi(0)/\mu_{eff}^2 \gamma(0) \tag{1}$$

where k_B is the Boltzmann constant. In an impurity Kondo system with spin $\frac{1}{2}$, $R = 2$ while, for a heavy-fermion system, it varies from magnetic ($R = 0.8$–1.2) through non-magnetic ($R = 0.56$–0.75) to superconducting ($R < 0.52$). In the present Ce_xSi_{100-x} alloys however, the concentration dependence of the $\chi(0)$-values conflicts with that of the $\gamma(0)$-values, probably owing to the abnormal behaviour of magnetic susceptibility, and the ratio R is abnormally large ($R \simeq 10$–40). The rapid rise in $\chi(T)$ towards low temperatures can be attributed to the presence of the Ce atoms which do not contribute to the Kondo effect, e.g. Ce^{3+} ions [19, 20]. The $\chi_{HF}(0)$-values estimated from the slopes of the magnetization curves at high magnetic fields are not appreciably different for measurements at 1.8 K and 4.2 K. So we assume that the high-field magnetic susceptibility $\chi_{HF}(0)$ is intrinsic. The Wilson ratio R estimated from the $\chi_{HF}(0)$-values has reasonable values as shown in table 1. In this context, we can estimate the concentration of Ce^{3+} ions carrying a magnetic moment from the spontaneous magnetization M_s obtained by extrapolating the slope at high fields to $H = 0$ kOe. The M_s-value of $0.6\mu_B$ implies that the present amorphous alloys have about 30% Ce^{3+} even at 4.2 K.

5. Conclusion

All the present Ce_xSi_{100-x} amorphous alloys show an extremely large electronic specific-heat coefficient at low temperatures, and are classified as heavy-fermion systems. The χ^{-1} versus T curves roughly obey the Curie–Weiss law with an effective Bohr magneton number of about $2.45\mu_B$ between 30 and 300 K. They deviate downwards from the straight line below 30 K and become nearly constant below 10 K. However, their electrical resistivities are dominated by disorder scattering, revealing a Kondo-type logarithmic temperature dependence. The atomic randomness suppresses the hybridization of 4f and conduction electrons and decreases the Kondo temperature, where about 30% of 4f electrons still have magnetic moments at low temperatures. The coherently ordered state such as a degenerate Fermi liquid and the magnetic ordered state observed in the crystalline counterparts are completely suppressed by the atomic randomness. In order to understand the detailed electronic structure, we are now carrying out an x-ray photoemission spectroscopy study. These results will be published elsewhere.

Acknowledgments

The authors wish to thank Professor H Fujimori for use of sputtering equipment, Dr G Kido for use of the magnetometer and Dr K Takada for his chemical analysis. They are indebted to the High Field Laboratory for Superconducting Materials, Tohoku University, for the magnetization and the magnetoresistance measurements. This work was supported partially by a Grant-in-Aid for Scientific Research on Priority Areas (grant 02216102) and a Grant-in-Aid for General Scientific Research (grant 03452029) given by the Ministry of Education, Science and Culture of Japan. It was also partially supported by the New Energy and Industrial Technology Development Organization.

References

[1] Stewart G R 1984 *Rev. Mod. Phys.* **56** 755, and references therein
[2] Grewe N and Steglich F 1991 *Handbook on the Physics and Chemistry of Rare Earths* vol 14, ed K A Gschneidner Jr and L Eyring (Amsterdam: Elsevier) p 343
[3] Brandt N B and Moshchalkov V V 1984 *Adv. Phys.* **33** 373
[4] Amano H, Sumiyama K, Suzuki T and Suzuki K 1991 *J. Phys. Soc. Japan* **60** 397
Suzuki K, Sumiyama K, Amano H, Yamauchi H and Suzuki T 1992 *J. Magn. Magn. Mater.* **108** 161
Sumyama K, Amano H, Yamauchi H, Suzuki K and Suzuki T 1992 *J. Phys. Soc. Japan* **61** 2359
[5] Sato N, Mori H, Satoh T, Miura T and Takei H 1988 *J. Phys. Soc. Japan* **57** 1384
Yashima H, Lin C F and Satoh T 1986 *Solid State Commun.* **57** 793
Yashima H, Sato N, Mori H and Satoh T 1982 *Solid State Commun.* **43** 595
Yahsima H and Satoh T 1982 *Solid State Commun.* **41** 723
[6] Malterre D, Durand J and Marchal G 1984 *J. Non-Cryst. Solids* **61–2** 1137
Materre D, Siari A, Durand J and Marchal G 1985 *J. Physique Coll.* **46** C8 205
[7] Hihara T, Sumiyama K, Yamauchi H, Suzuki T and Suzuki K 1991 *Solid State Commun.* **80** 749
[8] Hihara T, Sumiyama K, Yamauchi H, Suzuki T and Suzuki K 1993 *Physica* B **186** 466
[9] Kontani M, Senda M, Nakano M, Lawrence J M and Adachi K 1987 *J. Magn. Magn. Mater.* **70** 378
[10] Laborde O, Pierre J, Houssay E, Rouault A, Sénateur J P and Madar R 1990 *J. Low Temp. Phys.* **81** 171
Hill P, Willis F and Ali N 1992 *J. Phys.: Condens. Matter* **4** 5015
[11] Gschneidner K A Jr, Tang J, Dhar S K and Goldman A 1990 *Physica* B **163** 507
[12] Adrian G, Adrian H, Möhle W, Gerhäuser W, Lippert M, Hensel B and Niederhofer H 1988 *J. Magn. Magn. Mater.* **76–7** 642
Adrian G and Saemann-Ischenko G 1988 *Z. Phys.* B **72** 235
[13] Rauchschwalbe U, Steglich F, de Visser A and Franse J J M 1987 *J. Magn. Magn. Mater.* **63–4** 347
[14] Daybell M D 1973 *Magnetism* vol 5, ed H Suhl (New York: Academic) p 121
[15] Jan J-P 1958 *Solid State Physics* vol 5, ed F Seitz and D Turnbull (New York: Academic) p 1
[16] Fischer K H 1985 *Phys. Status Solidi* b **130** 13
[17] Ziman J M 1972 *Principles of the Theory of Solids* (Cambridge: Cambridge University Press) p 253
[18] Newns D M and Hewson A C 1980 *J. Phys. F: Met. Phys.* **10** 2429
Zou Z and Anderson P W 1986 *Phys. Rev. Lett.* **57** 2073
[19] Rauchschwalbe U, Baus W, Horn S, Spille H, Steglich F, de Boer F R, Aarts J, Assmus W and Herrmann M 1985 *J. Magn. Magn. Mater.* **47–8** 33
[20] Felsch W, Kushnir S G, Samwer K, Schröder H, van den Berg R and von Löhneysen H 1982 *Z. Phys.* B **48** 99